Supplement of Atmos. Chem. Phys., 15, 1367–1383, 2015
http://www.atmos-chem-phys.net/15/1367/2015/
doi:10.5194/acp-15-1367-2015-supplement

Atmospheric Chemistry and Physics Open Access

Supplement of

Size-resolved observations of refractory black carbon particles in cloud droplets at a marine boundary layer site

J. C. Schroder et al.

Correspondence to: A. Bertram (bertram@chem.ubc.ca)

S1. Procedure for calculating CVI$-D_{50}$

The CVI-D_{50} is the minimum droplet diameter for which the stopping distance (D_{stop}) is greater than the combination of CVI probe size and the distance between the CVI inlet and the internal stagnation plane (L_{stag}) and can be calculated based on the following equation:

$$CVI - D_{50} = D_{stop} > L_{stag} \quad \text{(S1)}$$

where L_{stag} is comprised of three components, and is equal to:

$$L_{stag} = L_{min} + L_{por} + L_{cur} \quad \text{(S2)}$$

where L_{min} is the amount of dead-space that exists between the CVI orifice and the top of the porous frit, L_{por} is the length from the top of the porous frit to the bottom of the stagnation plane, which is related to the counterflow (F1), sample flow (F2), and the length of the entire porous frit (X) by equation S3:

$$L_{por} = \left[\frac{F1-F2}{F1}\right] X \quad \text{(S3)}$$

L_{cur} is a parameterization (Anderson et al., 1993) that estimates the length a particle must traverse to deviate from the high velocity streamlines curving around the CVI probe tip in order to enter the CVI orifice, and is considered a linear function of the outer radius of the tip (r_o):

$$L_{cur} = Cr_o \quad \text{(S4)}$$

where C can range from 0 to 1 (Anderson et al., 1993; Noone et al., 1988) and represents the uncertainty of the estimate. In this study, CVI-D_{50} was reported at C = 0.5 and the uncertainty was calculated by averaging the differences calculated when using the lower and upper bounds of C = 0 and C = 1, respectively.

D_{stop} can be calculated as follows (Serafini, 1954):

$$D_{stop} = \frac{r_d \rho_d}{3\varepsilon^{\frac{3}{2}} \rho_{air}} \left[Re_d^{\frac{1}{3}} \varepsilon^{\frac{1}{2}} - \frac{\pi}{2} + tan^{-1}\left(Re_d^{\frac{-1}{3}} \varepsilon^{\frac{-1}{2}} \right) \right] \quad \text{(S5)}$$

where r_d is the droplet radius, ρ_d is the droplet density, ε is a constant (0.158), ρ_{air} is the density of air, and Re_d is the droplet Reynolds number, which is represented by:

$$Re_d = \frac{2\rho_d r_d V_\infty}{\eta_{air}} \quad \text{(S6)}$$

where V_∞ is the CVI air intake velocity and η_{air} is the viscosity of air. The calculation needed to determine the CVI enhancement factor (EF) is:

$$EF = \frac{V_\infty \pi r_i^2}{F2} \quad \text{(S7)}$$

S2. SP2 size-dependent correction factors

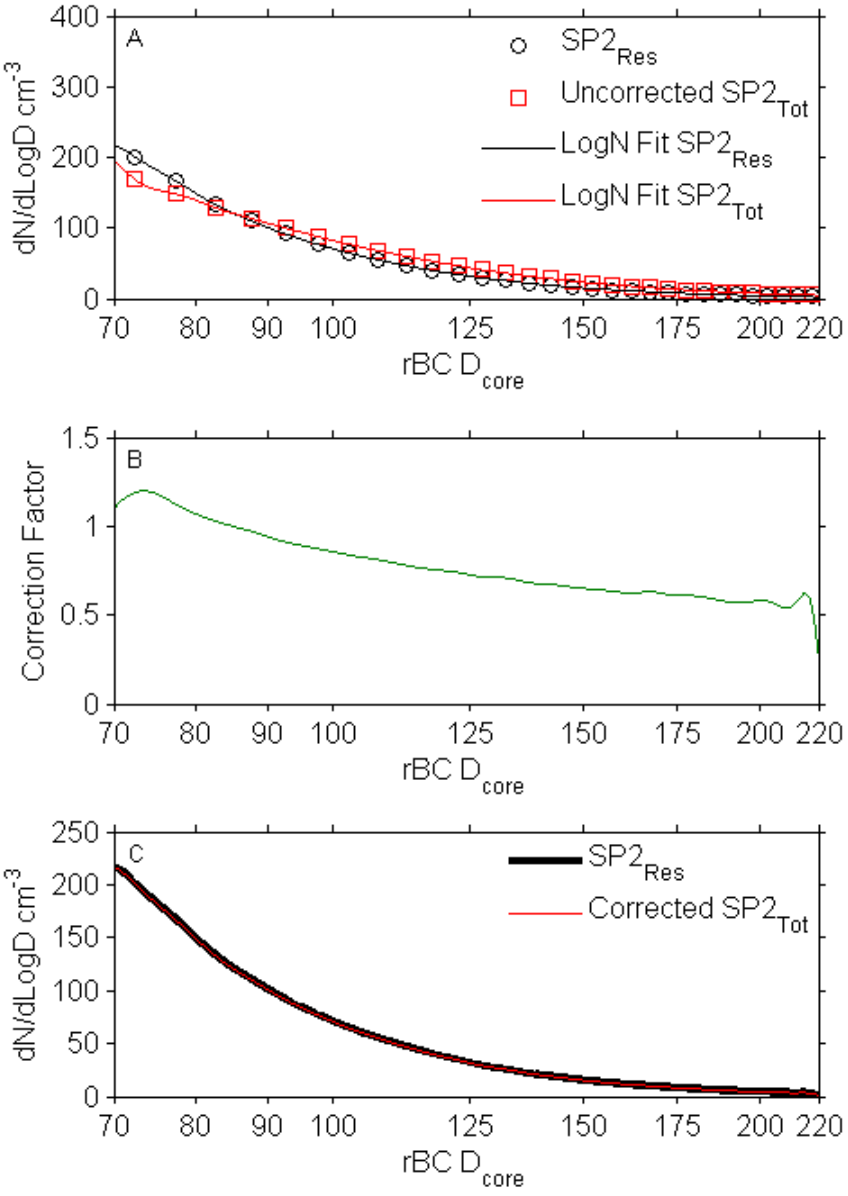

Fig. S1. Demonstration of the SP2 size dependent instrument sensitivity correction factor calculation. Panel A shows the number distributions from both the $SP2_{Res}$ (black circles) and the $SP2_{Tot}$ (red squares) each with the corresponding lognormal fits (lines) from ambient cloud-free data; panel B shows the ratio of the $SP2_{Res}$ to the $SP2_{Tot}$, which is used as the correction factor at each size; and panel C shows the distributions after the correction factor has been applied.

S3. Calculated coagulation rates between rBC particles and cloud droplets

The fraction of particles incorporated into cloud droplets by coagulation can be calculated by considering an evenly distributed population of rBC-containing particles surrounding the cloud droplets. In this case, since the mean free path of the rBC-containing particles is much smaller than the diameter of the droplets (mean free path on the order of 1.5 x 10^{-2} µm), calculations are done for the continuum regime and the Brownian coagulation coefficient , K (in $m^3 s^{-1}$), is given by equation S8 (Seinfeld and Pandis, 2006):

$$K = \frac{2kT}{3\eta_{air}} \cdot \frac{\left(D_{rBC} + D_{droplet}\right)^2}{D_{rBC} D_{droplet}} \quad \text{(S8)}$$

where k is the Boltzmann constant, T is temperature, η_{air} is the viscosity of air at temperature T, and D_{rBC} and $D_{droplet}$ are the diameters of the rBC-containing particles and droplets respectively.

The coagulation rate (in $m^{-3} s^{-1}$) can be calculated by multiplying the number concentration of rBC-containing particle and droplets by the coagulation coefficient:

$$J = K \cdot N_{rBC} \cdot N_{droplet} \quad \text{(S9)}$$

From this, the fraction of rBC-containing particles incorporated into cloud droplets by coagulation can be calculated by multiplying the coagulation rate by the droplet residence time and dividing by the total number concentration of rBC-containing particles:

$$F_{coagulated} = \frac{J \cdot t_{residence}}{N_{rBC}} \quad \text{(S10)}$$

Sizes and number concentrations of the rBC containing particles and droplets were measured during the campaign. Number concentrations for droplets greater than CVI– D_{50} were on the order of 25-35 cm^{-3} while number concentrations for the smallest rBC cores (70-80 nm diameter) were on the order of 21-26 cm^{-3}. rBC number concentrations decreased with increasing core size to a minimum of

0.10-0.13 cm^{-3} for the largest core sizes (210-220 nm diameter). Median cloud droplet diameters were ~30 µm (see Table S1 for details).

Table S1. Measured parameters used in coagulation calculations.

		Cloud 2	**Cloud 3**
Number concentration of droplets greater than the CVI-D_{50} (cm^{-3})		25.715	34.992
Median droplet diameter (µm)		30.74	30.8
Average Temperature (K)		286.6	288.4
Number concentration of rBC cores (cm^{-3})	70 - 80 nm	21.026	26.616
	80 - 90 nm	13.269	13.363
	90 - 100 nm	8.7397	7.6413
	100 - 110 nm	6.2334	4.569
	110 - 120 nm	4.1541	2.7838
	120 - 130 nm	2.7786	1.7634
	130 - 140 nm	1.9505	1.1626
	140 - 150 nm	1.3068	0.7675
	150 - 160 nm	0.94837	0.55232
	160 - 170 nm	0.72862	0.39462
	170 - 180 nm	0.53827	0.28741
	180 - 190 nm	0.44935	0.21798
	190 - 200 nm	0.30142	0.15744
	200 - 210 nm	0.19267	0.1275
	210 - 220 nm	0.13775	0.10572

Although stratocumulus decks can persist for hours, large eddy simulations of non-precipitating stratocumulus suggest that in-cloud residence times of air parcels can be on the order of 12 minutes

(Stevens et al., 1995). Based on this work, we assume that an upper limit of 1 hour for the clouds measured in this study is reasonable.

Based on these parameters, the fraction of rBC particles incorporated into the cloud droplets is calculated to be less than 0.8% for 75 nm rBC particles. In Fig. S2 we show the fraction of rBC particles that will be incorporated into cloud droplets as a function of rBC particle size. For these calculations we assume diffusion in the continuum regime and use the measured parameters given in Table S1. This figure shows that the fraction of rBC particles that will be incorporated into cloud droplets should be a strong function of size, and for 200 nm rBC particles the fraction incorporated will be <0.3%. These calculations assume the rBC particles have no coatings. If they have coatings, then the fraction incorporated into cloud droplets by coagulation will be even lower.

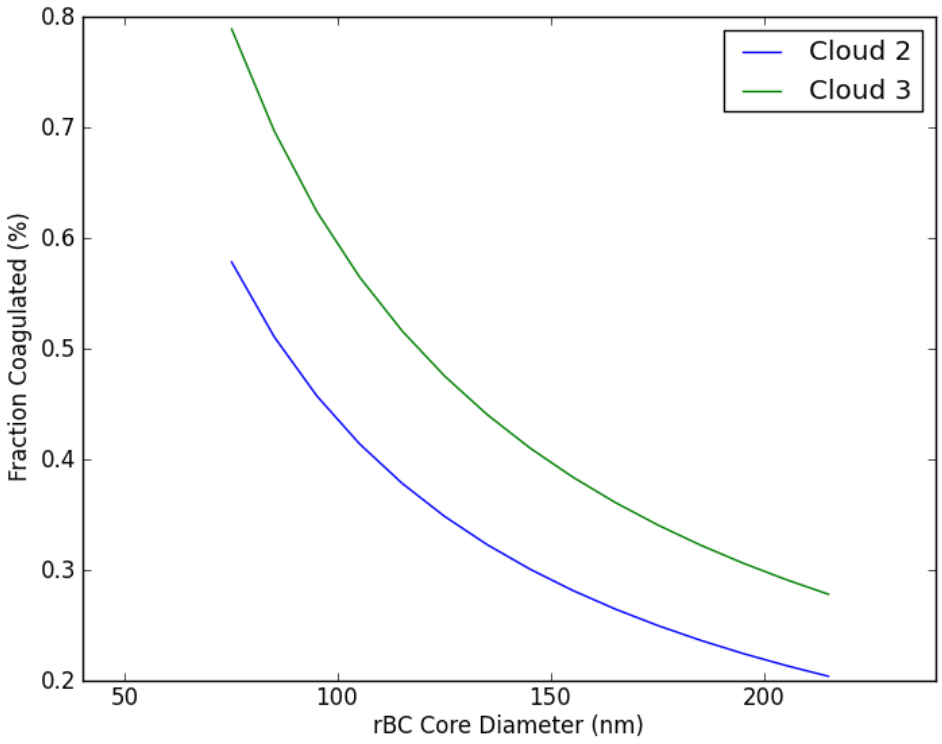

Fig. S2. Fraction of rBC cores incorporated into cloud droplets by coagulation over a 1 hour period as a function of rBC core diameter. Parameters used for the calculations are given in Table S1.

S4. Determination of the droplet transmission in the CVI

The droplet transmission factor (DT) through the CVI was determined by plotting the number of droplets measured by the FM-100 that were greater than the CVI-D_{50} as a function of the number of residual particles (see Figure S3). The number of residual particles plotted in Fig. S3 were corrected for the CVI enhancement factor (EF) and only residual particles > 100 nm were included since particles smaller than this size were likely not present due to nucleation scavenging (see Sect. 3.3.2 in manuscript for further discussion). From 1/slope in Fig.S1a and b, the DT values were determined to be 26% during Cloud 2 and 45% during Cloud 3. DT values less than 100% may be attributed to; (1) particle or droplet losses in the CVI, (2) incomplete drying of the droplets, (3) misalignment of droplets in the wind tunnel prior to entering the CVI, and (4) insufficient acceleration of some of the larger droplets.

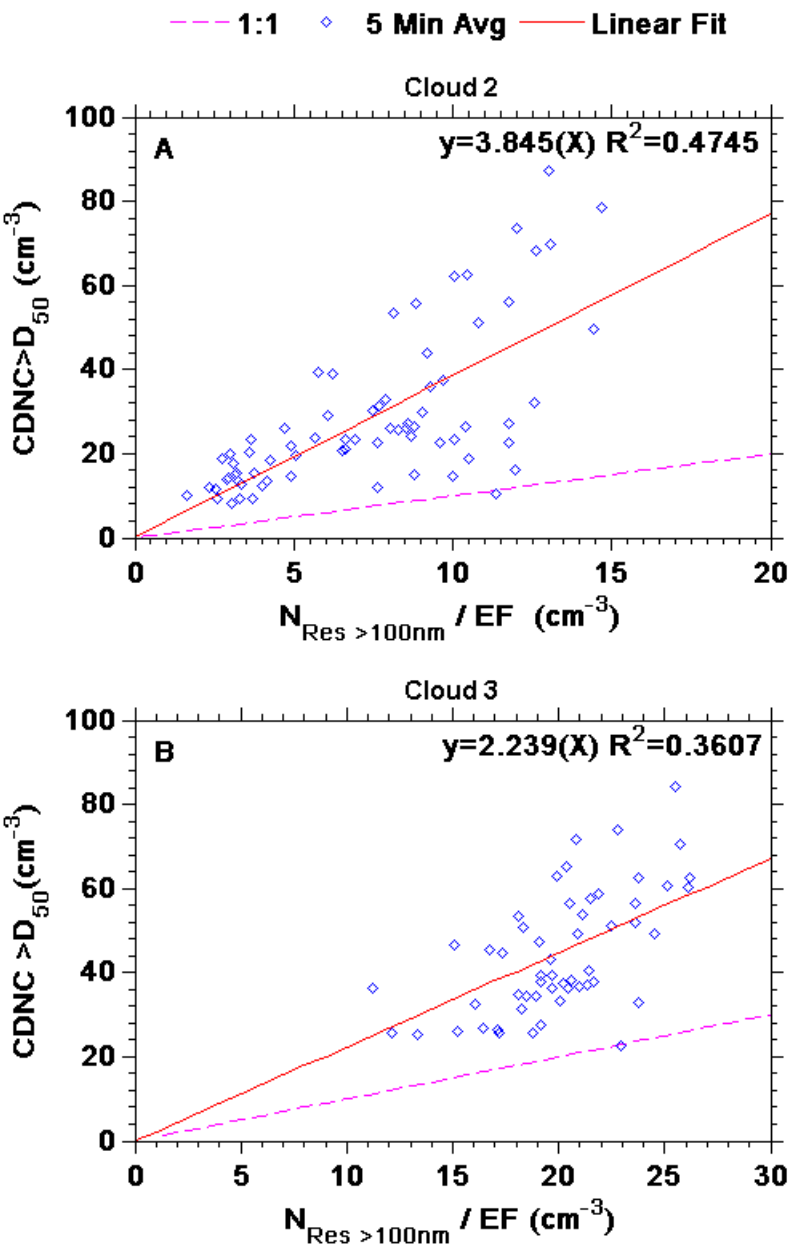

Fig. S3. Correlation plots between the cloud droplet number concentration (CDNC) greater than the CVI-D_{50} (CDNC > D_{50}) and the enhancement (EF) corrected residual number concentrations greater than 100nm ($N_{Res>100nm}$) in cm^{-3}.

S5. AMS ion pairing scheme

The inorganic ions (NH_4^+, NO_3^-, SO_4^{2+}, Cl^-) mass fractions measured with the HR-ToF-AMS were converted to mass fractions of ammonium nitrate, ammonium sulfate, ammonium bisulfate, sulfuric acid, or ammonium chloride using the simplified ion pairing scheme below:

$$n[NH_4NO_3] = n[NO_3^-]$$

$$n[NH_4Cl] = n[Cl^-]$$

$$n[(NH_4)_2SO_4] = \max(0, n[NH_4^+] - n[SO_4^{2+}] - n[NO_3^-] - n[Cl^-])$$

$$n[NH_4HSO4] = \min(2n[SO_4^{2+}] - n[NH_4^+] + n[NO_3^-] + n[Cl^-], n[NH_4^+] - n[NO_3^-] - n[Cl^-])$$

$$n[H_2SO_4] = \max(0, n[SO_4^{2+}] - n[NH_4^+] + n[NO_3^-] + n[Cl^-])$$

where *n* is the number of moles of that species. This ion scheme is the same as the one used by Gysel et al., 2007 except that it has been modified to incorporate ammonium chloride.

References:

Anderson, T. L., Charlson, R. J. and Covert, D. S.: Calibration of a Counterflow Virtual Impactor at Aerodynamic Diameters from 1 to 15 μm, Aerosol Sci. Technol., 19(3), 317–329, 1993.

Gysel, M., Crosier, J., Topping, D. O., Whitehead, J. D., Bower, K.N., Cubison, M. J., Williams, P. I., Flynn, M. J., McFiggans, G.B., and Coe, H.: Closure study between chemical composition and hygroscopic growth of aerosol particles during TORCH2, Atmos. Chem. Phys., 7, 6131–6144, doi:10.5194/acp-7-6131-2007, 2007.

Noone, K. J., Ogren, J. a., Heintzenberg, J., Charlson, R. J. and Covert, D. S.: Design and Calibration of a Counterflow Virtual Impactor for Sampling of Atmospheric Fog and Cloud Droplets, Aerosol Sci. Technol., 8(3), 235–244, 1988.

Seinfeld, J. H. and Pandis, S. N.: Atmospheric Chemistry and Physics: From Air Pollution to Climate Change, 2nd ed., John Wiley & Sons, Hoboken, NJ., 2006.

Serafini, J. S.: Impingement of water droplets on wedges and double-wedge airfoils at supersonic speeds, NACA, TR 1159, 1954.

Stevens, B., Feingold, G., Cotton, W. R. and Walko, R. L.: Elements of the Microphysical Structure of Numerically Simulated Nonprecipitating Stratocumulus, J. Atmos. Sci., 53(7), 980–1006, 1995.